

NuMI Target Vibration Measurements

Robert G. Wagner
Argonne National Laboratory, Argonne, Illinois 60439

April 16, 2004

Abstract

The NuMI target exhibits vibration with a very long damping time. The vibration of the target is easily excited due to its long length and narrow cross section. This situation gives the potential for a variety of environmental conditions to excite resonant vibration of the target. These include focusing horn pulsing, high speed cooling air flowing, and cooling water flowing through the target. Measurements have been made of vibration excited by horn pulsing and by air and water flow from a setup designed to mimic that of the target hall environment. None of the conditions excites large or resonant vibration in the target. Also discussed are measurements of the fundamental vibration frequencies of the target and attempts to produce a simulation of these vibrations.

1 Introduction

The NuMI beam production target is composed of a series of forty seven 20mm long graphite sections brazed to stainless steel cooling water tubes on the upper and lower edges of the graphite [1]. The thickness of the graphite segments is 6.4 mm and spacing between segments is 0.3mm. This composition leads to a very long ($\sim 1m$) thin cantilever that is easily excited into vibration. Vibration of a few millimeters amplitude would cause the beam flux intercepting the target to vary in a complicated and potentially uncalculable manner. The vibration could also lead to the undesirable situation of the target vacuum shell hitting the inner conductor of NuMI horn 1 in the low energy configuration with the target inserted within the horn 1 inner volume. In order to determine if these were actual problems, measurements were made of the target vibration under various environmental conditions:

1. Exciting vibration of the free standing target. A rubber hammer was used to hit the support plate for the target to induce the vibration. A ball bearing rolled through a length of PVC pipe to strike the support plate was also used in order to give a more reproducible excitation.
2. Pulsing of the NuMI horn 1 prototype with the target inserted at its nominal low energy position within the horn.
3. Using large exhaust fans to simulate the approximately 9 m/s air flow past the target. The target vibration was measured with the target both inside and outside the prototype horn 1. Later the vibration was remeasured with the target mounted in the target/baffle carrier structure.
4. Cooling water flowing through the stainless steel support lines to which the graphite sections are attached.

I describe in the remainder of the note the experimental apparatus used to measure vibration, the results of the various measurements listed above, calculation of the vibrational modes of the target, simulation of the observed vibration modes, and conclusions as to the effect of vibration on the ability to operate with the target inside focusing horn 1.

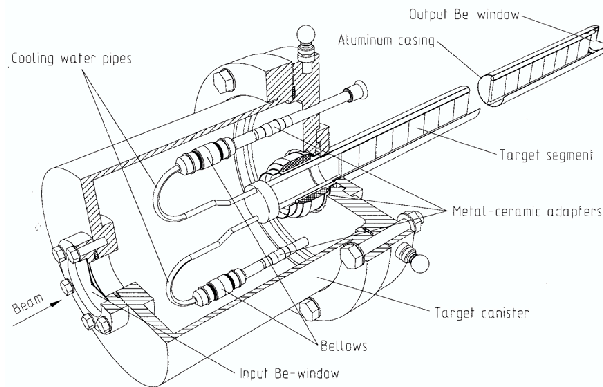


Figure 1: Target overview schematic from the NuMI Technical Design Handbook. Components relevant to the vibration measurements are discussed in the text.

2 Vibration Measurement Apparatus

The apparatus used for target vibration measurements is a non-contact position sensor consisting of a photodiode whose emitted light is detected by a phototransistor. A small brass vane is attached to the device whose vibration is to be measured. The photodiode/phototransistor combination is positioned so that the vane intercepts a portion of the light emitted by the photodiode. The current from the phototransistor then is a function of how much of the light is eclipsed by the vane. The apparatus was constructed by Frank Nezrick and is called an eclipsometer. The phototransistor output is quite sensitive to any change in the amount of light it sees from the photodiode and has a resolution of 1V per 0.12mm of movement of the vane with respect to the stationary photodiode/phototransistor pair. The eclipsometer has a linear response over approximately 3V. Thus, it is useful for measurements with a full amplitude of only about 0.36mm. The eclipsometer is typically positioned with respect to the brass vane so that the quiescent voltage is 1.6-1.8V, i.e. approximately at the midpoint of its linear region.

The brass vane is mounted on the device to be measured with a small amount of wax. I used both beeswax and a product called Tacky Wax to mount the vane on the target. Tacky Wax is easily available in hobby and craft stores that sell candle making supplies.

The voltage output of the phototransistor was recorded with a Hewlett-Packard Dynamic Signal Analyzer that allowed viewing either the absolute voltage as a function of time (denoted time domain hereafter) or the fourier transformed frequency spectrum (denoted frequency domain hereafter). This allows determination of both the absolute scale of physical vibration of the target and also a quick estimation of the main frequencies of vibration excited within the target. The Dynamic Signal Analyzer is an older model and the only method of permanently recording the data is using a pen plotter to record the DSA displays.

3 Target Description

Although description of the target is available in the NuMI Technical Design Handbook [1], I describe briefly here the construction of the target and reproduce the target schematics from figures 4.2-12 and 4.2-13 of the Handbook for the convenience of the reader.

A copy of figure 4.2-12 is shown as figure 1. The downstream plate of the target canister through

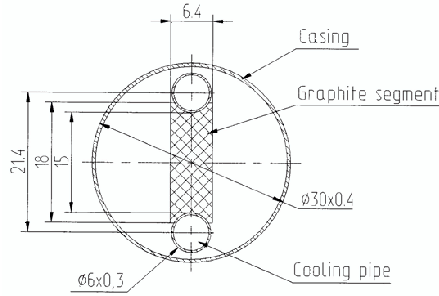


Figure 2: Beam view of target cross section. Dimensions are given in millimeters.

which the aluminum casing of the target core protrudes is used to reference the distance along the aluminum casing at which target vibrations were measured. The brass vane of the eclipsometer system was attached using wax to the aluminum casing. The most downstream graphite target segment ends approximately 95cm from the target canister downstream plate. The stainless steel tubes that form the upper and lower supports for the graphite segments are shown as they exit from the target core into the target canister and bend through 180° to exit the canister above and below the aluminum casing. A beam's eye view of the target is shown in figure 2 which is a reproduction of Handbook figure 4.2-13. The graphite is seen to have a minimum vertical dimension of 15mm and to curve around the stainless steel cooling tubes to a maximum vertical extent of 18mm. The 6.4mm thickness of the graphite transverse to the beam is noted. The thinness of the target allows easy vibration in the horizontal plane. The presence of the stainless steel tubes and the height of the graphite segments give more stiffness in the vertical plane where any vibration is much reduced and damps quickly.

4 Vibration Measurements on Free Standing Target

I now begin a description of the various measurement setups and observed vibrations both in absolute spatial size and frequency components. In this section are described measurements made on the “free standing” target to determine the resonant frequencies of the target and their damping times. We'll then take a diversion to discuss calculation of the resonant frequencies using a cantilever model. Then we'll return to measurements made of vibration with the target inserted in horn 1 and installed on the target carrier framework.

What I call the free standing target consisted of the whole of the target including its vacuum and cooling assemblies attached to an aluminum mounting plate to allow the target to sit freely on a flat surface in its nominal horizontal position. The aluminum mounting plate consisted of a 0.5” thick aluminum base plate welded at right angles to a second 0.5” thick aluminum plate to which the target was bolted. By striking the mounting plate with either a rubber hammer or a 1” diameter ball bearing rolled through a PVC pipe, vibration was excited in the target and the size, resonant frequency, and damping time measured using the eclipsometer system.

The first measurements were made using a rubber hammer to excite the vibration. What was really needed though was an estimate of the variation of vibration amplitude along the length of the target. When the target was inserted into the focusing horn, most of the target was not accessible to vibration measurement and only about 30cm extending beyond the target canister could be seen. Since the largest amplitude of vibration would be at the end of the target, it was necessary to predict the vibration at this point by measuring it at a point nearer the base of the target.

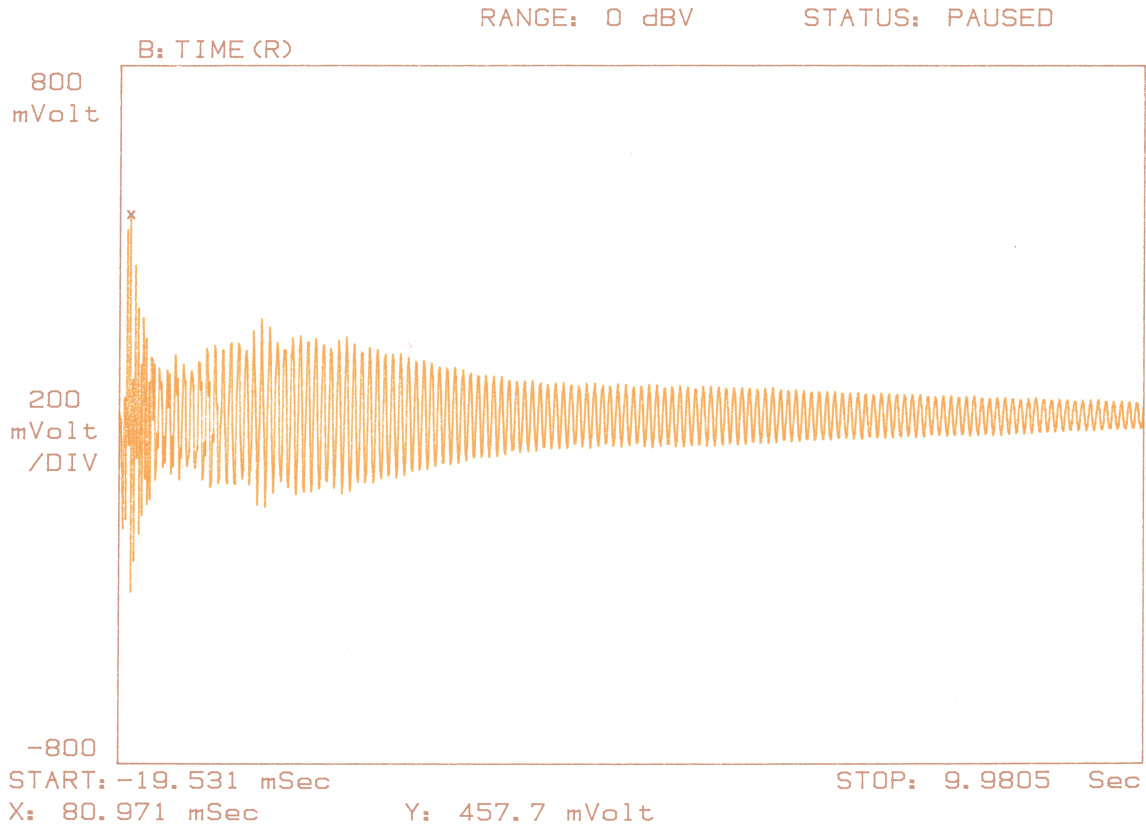


Figure 3: Target vibration measured 29 cm downstream of target canister. Vibration was excited by rolling a 1" diameter ball bearing through the full length of a 62" PVC pipe set at a fixed angle with respect to the horizontal. The vertical scale is the output of the eclipsometer in mV with 100mV corresponding to a deflection of 0.012mm. Recording of the display was triggered using an internal trigger for the dynamic signal analyzer set with a low threshold to inhibit triggering on noise but sensitive to the vibration induced by the ball bearing striking the mounting plate.

To make this inference, it was necessary to excite the vibration in a reproducible way. I chose to do this using a 1 inch ball bearing rolled through a length of PVC pipe and striking the target mounting plate. Results from these measurements are shown in figures 3-5. The depictions of vibration shown in these figures are used throughout the remainder of the note; so I describe briefly the horizontal and vertical scales. For the time domain plots, time is shown on the horizontal scale in seconds. The time extent is typically 10s, but an 800ms extent is used for showing results from horn pulsing. For a triggered display, the display is shown from about 20ms before the trigger for easier viewing of the early vibration. The vertical scale for time domain plots is in volts where 100mV corresponds to a displacement of the target by 0.012mm. The pen plotter allows marking a chosen location along the plot trace with an "X". For figures 3-5, the mark is made at the location of the largest displacement of the target: $\sim 0.055\text{mm}$ for the 29cm point, $\sim 0.071\text{mm}$ for the 59cm point, and $\sim 0.175\text{mm}$ for the 100cm point. The frequency domain plots show frequency in Hertz on the horizontal scale starting at 0 and extending to 40-200Hz. The vertical scale is relative and is in dBV. The minimum and maximum of the vertical scale are shown on the left hand side of the scale. The dB/division is irrelevant since the pen plotter does not draw the vertical grid. I've have noted the main observed frequency components on most frequency domain plots.

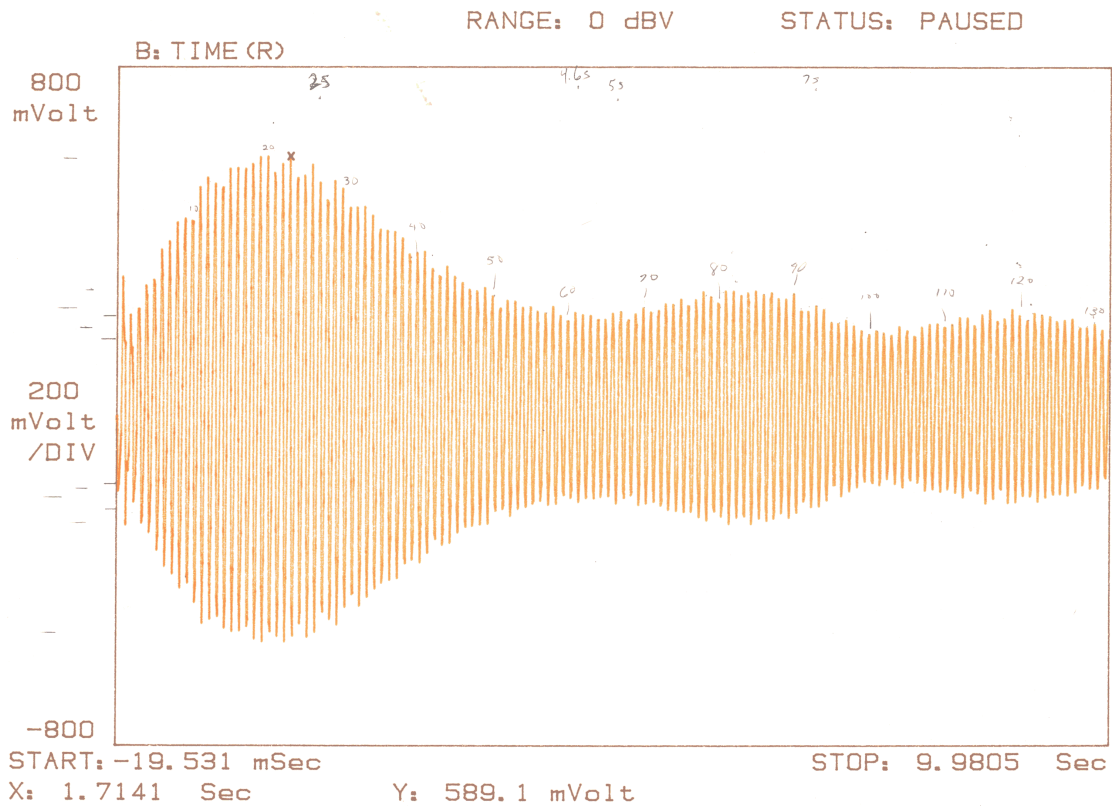


Figure 4: Target vibration measured 59 cm downstream of target canister. Other than the location measured along the target all other setup is the same as figure 3.

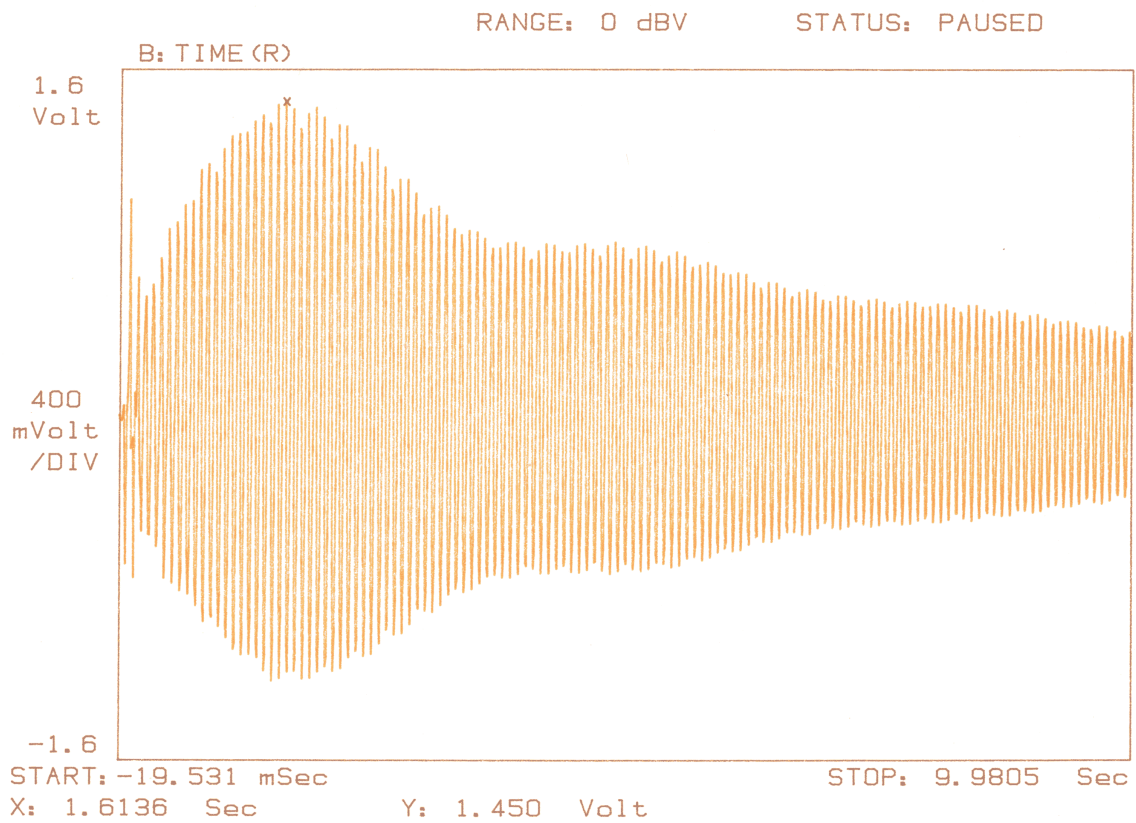


Figure 5: Target vibration measured 100 cm downstream of target canister. Other than the location measured along the target all other setup is the same as figure 3. The location corresponds to the downstream end of the target.

As expected the amplitude of vibration increases with distance from the target canister. The increase is non-linear and the frequency components present depend on location along the target. For the purpose of inferring the vibration at the end of the target from the 29 cm measurement, we use a scale factor of 7. This allows us to estimate the vibration at the end of the target when it is fully inserted into horn 1. The scale factor disregards the large initial relative deflection at the 29 cm point and uses the first maximum of the beat pattern seen at about 1.5s.

As is evident in the preceding figures, a number of frequency components are present in the vibration. The dynamic signal analyzer used to record the measurements has a fast Fourier transform option to display the frequency domain spectrum of the data. In order to observe higher frequency components of the vibration spectrum, the time scale was reduced to 2s. This allows observation of frequencies up to 200Hz. This covers the range of frequencies with significant contributions. Frequency domain spectra for the 29cm and 100cm positions are shown in figure 6. The main resonant frequency is 13Hz to 13.5Hz. While harmonics of 13Hz are visible near 26 and 39Hz, the main secondary harmonic is around 81.5Hz. As is discussed in the next section, this corresponds to the predicted value if the target is analyzed as a cantilever. Simulation of the vibrational modes is discussed in a later section and we find that all but the 13Hz fundamental vibration quickly damp out. The beat pattern evident in the time domain figures indicates a second frequency near 13Hz modulating the main vibrational mode.

4.1 Damping Time of Vibration

In an early measurement in which I excited the free standing target vibration by striking the mounting plate with a rubber hammer, I allowed the higher frequency components to damp out and then measured the damping time of the 13Hz component. I recorded a 10s time display from an eclipsometer measurement 29cm downstream of the target canister and used the Dynamic Signal Analyzer cursor to measure the amplitude of vibration at a number of time points. The best fit to the form $\exp(-t/\tau)$ gives $\tau = 12 \pm 1$ s. In section 7 where the simulation of the vibration of the free standing target is discussed, a decay time of 43.4s gives a good representation for the main frequency at 13.19Hz measured 59cm from the target canister. This latter damping time may be longer due to the location along the target (farther from the canister), simulating from the onset of the vibration rather than at a late time, both or neither. As I'll discuss in that section, a damping time near 12s would not give a good simulation of the 59cm measurement.

5 Calculation of Target Vibration Frequencies Using a Cantilever Model

The equation of motion of a beam [2] is

$$\frac{\partial^2 s}{\partial t^2} + a^2 \frac{\partial^4 s}{\partial x^4} = 0 \tag{1}$$

where $s(x, t)$ is the lateral displacement at position x along the beam at time t , and $a^2 \equiv EI/\mu$. Here, E is the Young's modulus of the beam material, I is the second moment of area of the beam, and μ is the mass per unit length of the beam. $I = bd^3/12$, where b is the width of the beam and d is the thickness. The NuMI target is composed of 47 sections of 20mm long graphite brazed to upper and lower stainless steel cooling tubes. Each 20mm section is separated from its neighbor by 0.3mm. The tubes are a distance of 15mm apart as shown in figure 2. So for our case, $b = 15mm$ and $d = 6.4mm$, where the latter is the thickness of a graphite section. The graphite

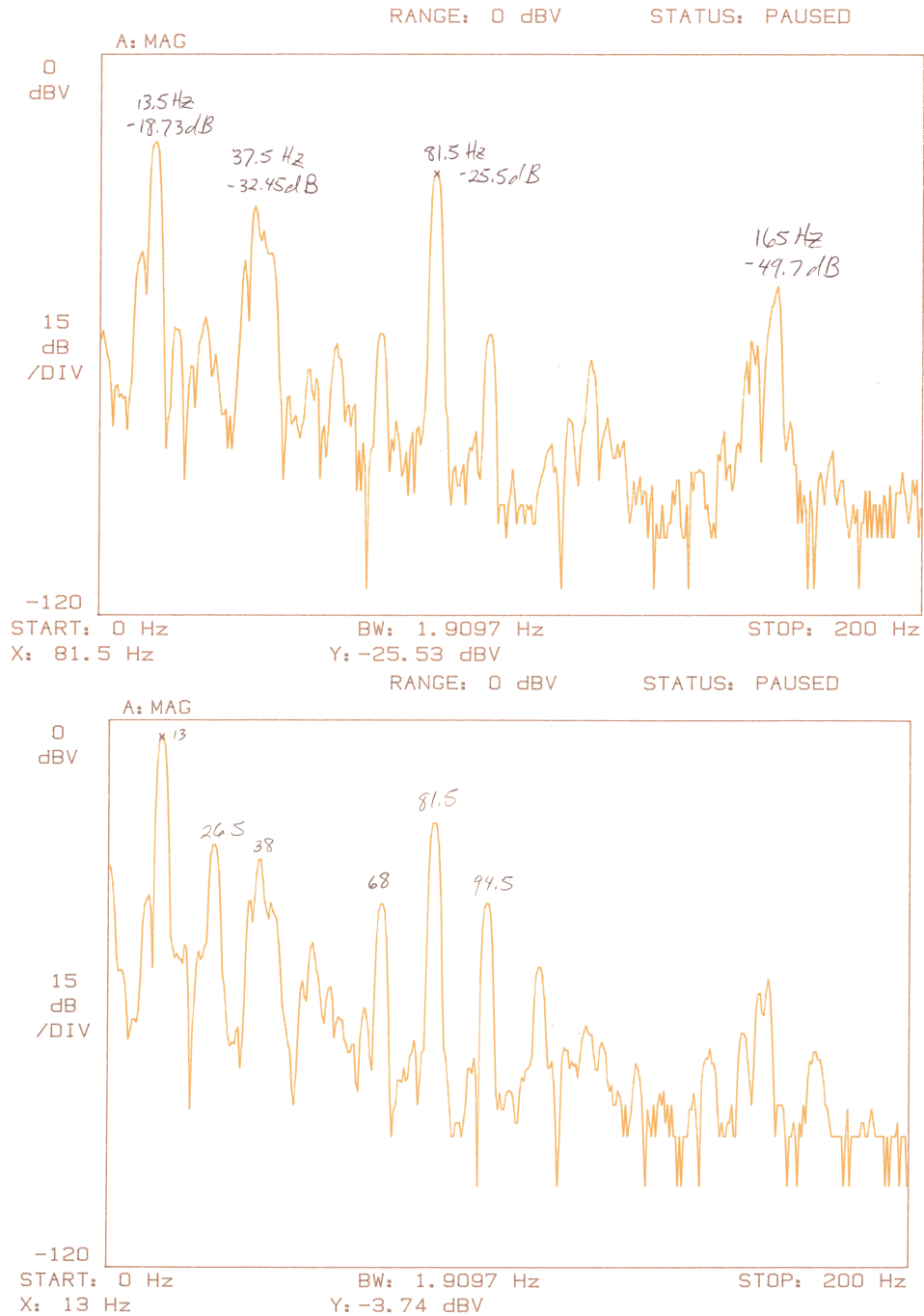


Figure 6: Frequency spectra measured for free standing target with vibration excited by a ball-bearing rolled into the mounting plate. The upper plot is for the measurement 29cm from the target canister and the lower plot is for the measurement at 100 cm from the target canister.

used has a density of $1.78g/cm^3$ which gives $\mu = 0.171g/mm$. The composite nature of the target makes calculation of Young's modulus quite difficult. However, we will see that measurement of the fundamental mode of vibration not only predicts the secondary modes, but also gives a reasonable estimate of the Young's modulus. The distance and time-dependent terms are assumed to separate to give

$$s(x, t) = X(x)e^{i\omega t}.$$

The general solution for $X(x)$ is

$$X(x) = A_1 \cosh kx + A_2 \sinh kx + A_3 \cos kx + A_4 \sin kx$$

where $k = \sqrt{\omega/a}$, $\omega = 2\pi f$. With the target fixed at $x = 0$ where its first derivative with respect to x is also zero, and assuming the bending moment and shear force vanish at the free end; we end up with four coupled equations. The determinant of the coefficients must vanish for a non-trivial solution for A_{1-4} . This ultimately leads to the condition that we find values of k that satisfy

$$\cosh k\ell \cos k\ell + 1 = 0$$

where $\ell \equiv$ length of target = 953.8mm. Turvey *et al.* give the first four roots as

$$k\ell = 1.8751, 4.6941, 7.8548, 10.9955.$$

Using the relation between k and the vibration frequency, f , we have

$$f = \frac{(k\ell)^2}{2\pi} \sqrt{EI/\mu\ell^4} \tag{2}$$

$$f_m = C_m \sqrt{EI/\mu\ell^4}, \quad C_m = \frac{(1.8751)^2}{2\pi}, \dots = 0.5596, 3.5069, 9.8195, 19.2420, \dots \tag{3}$$

The best estimate of the fundamental frequency is $f_1 = 13.19\text{Hz}$. The ratio of the first and second vibrational resonances is given by

$$f_2/f_1 = C_2/C_1 = 6.2668 \implies f_2 = 82.66\text{Hz}. \tag{4}$$

This agrees fairly well with the observed secondary of around 81.5Hz. Using equation 2 and solving for the Young's modulus, E , we find $E = 23.5\text{GPa}$ for the target. In comparison, the bulk graphite has a Young's modulus of around 14.5GPa as quoted on the Poco Graphite web site [3]. The higher value inferred for the target is likely a combination of ignoring the small amount of graphite beyond the 15mm height that wraps around the stainless steel tubes and the tubes themselves that stiffen the target cantilever.

6 Vibration Measurements in Simulated Beam Environments

6.1 Vibration Measurement During Horn 1 Pulsing

In order to measure the vibration during horn pulsing with the target fully inserted into the horn 1 prototype, the target was mounted onto a 3 axis transporter previously used for magnetic field mapping of the horn. The target was surveyed to be centered with respect to the central bore of the horn and its distance from the horn end cap measured in what was called the fully withdrawn position. The 3 axis transporter is equipped with a computer controlled positioning system that was used to accurately insert the target into the horn. The horn was then pulsed at full amplitude and

the vibration of the target measured for two positionings of the target within the horn: first with the target 10.11cm upstream of its nominal low energy position and secondly with the target fully inserted to its nominal low energy position. The first measurement was done as a safety check to make sure the target was not vibrating a lot during horn pulsing, i.e. we wanted to make sure we weren't going to vibrate the target can into contact with the horn inner conductor. The vibration was measured with the eclipsometer location fixed with respect to the horn so that we attached the brass vane at two locations along the target can: 25.7cm and 15.5cm from the target canister for a partially inserted and fully inserted target, respectively. Recall that one of the free standing measurements was 29cm from the target canister so we have an approximate way of inferring the vibration at the downstream end of the target.

In the partially inserted position, I measured a maximum amplitude of vibration of less than $2.5\mu\text{m}$. With this assurance of essentially negligible vibration during horn pulsing, the target was fully inserted and the vibration measured during pulsing was observed to be again less than $2.5\mu\text{m}$. Note that this implies that the vibration at the downstream end of the target is less than 0.02mm. The clearance between the aluminum target casing and the horn inner conductor is about 2.5mm. Figure 7 shows the time domain plot of the vibration using a signal from the horn current function generator to trigger the dynamic signal analyzer. The transient induced at the time of the horn pulse is evident. The vibration after the pulse is indistinguishable from that before the pulse. Whether the transient is electrical pickup by the eclipsometer signal line or an actual movement of the target is unknown. Since the signal represents negligible movement, the source of the transient was not traced.

6.2 Vibration Measurement with Air Flow

The flow of cooling air in the NuMI target hall will correspond to a wind with speed about 8.9m/s. With the surrounding shielding, the target will be enclosed on all sides. To simulation this environment, the target carrier framework was enclosed in plywood on the bottom and with clear, hard plastic on the sides and top. All edges were sealed with duct tape. Two large exhaust fans were mounted at the upstream end of the target carrier framework; one on top of the other. The target canister at the upstream end has diameter 16 cm and represents a large impedance to air flow in the region of the target core downstream. With both fans on, the airflow was measured at various locations at the downstream end of the target carrier. Near the aluminum target casing, the flow was ~ 2.5 m/s. The maximum flow was in the bottom beam right area where the air speed was ~ 7.1 m/s. Although this is less than the nominal and is especially low in the target region, the flow probably represents a good approximation of the target hall conditions. That is, the target canister will cause a dead region for flow around the target core in any configuration. However, to determine a "worst" case scenario, some plywood pieces were inserted as a baffle in the bottom of the target carrier and were oriented so as to direct air flow up toward the target. The target was originally mounted into the target carrier incorrectly so that it was rotated 90° from its nominal orientation, i.e. the stainless steel cooling water tubes with the 15mm wide graphite sections between them formed a horizontal rather than a vertical plane. This actually turned out to be fortunate as it allowed measurement of the vertical vibration resonant mode of the target. The vibration was measured ~ 3 cm from the downstream end of the target shell. The frequency domain plot is shown in figure 8. The horizontal fundamental frequency at 13.4Hz is visible, but the larger amplitude vibration mode observed was the 18.2Hz one corresponding to up and down motion of the target (when it is correctly mounted).

The target was then rotated to near the correct orientation. At the time of this first air flow measurement, the target could not be oriented with the graphite sections in a vertical plane, but

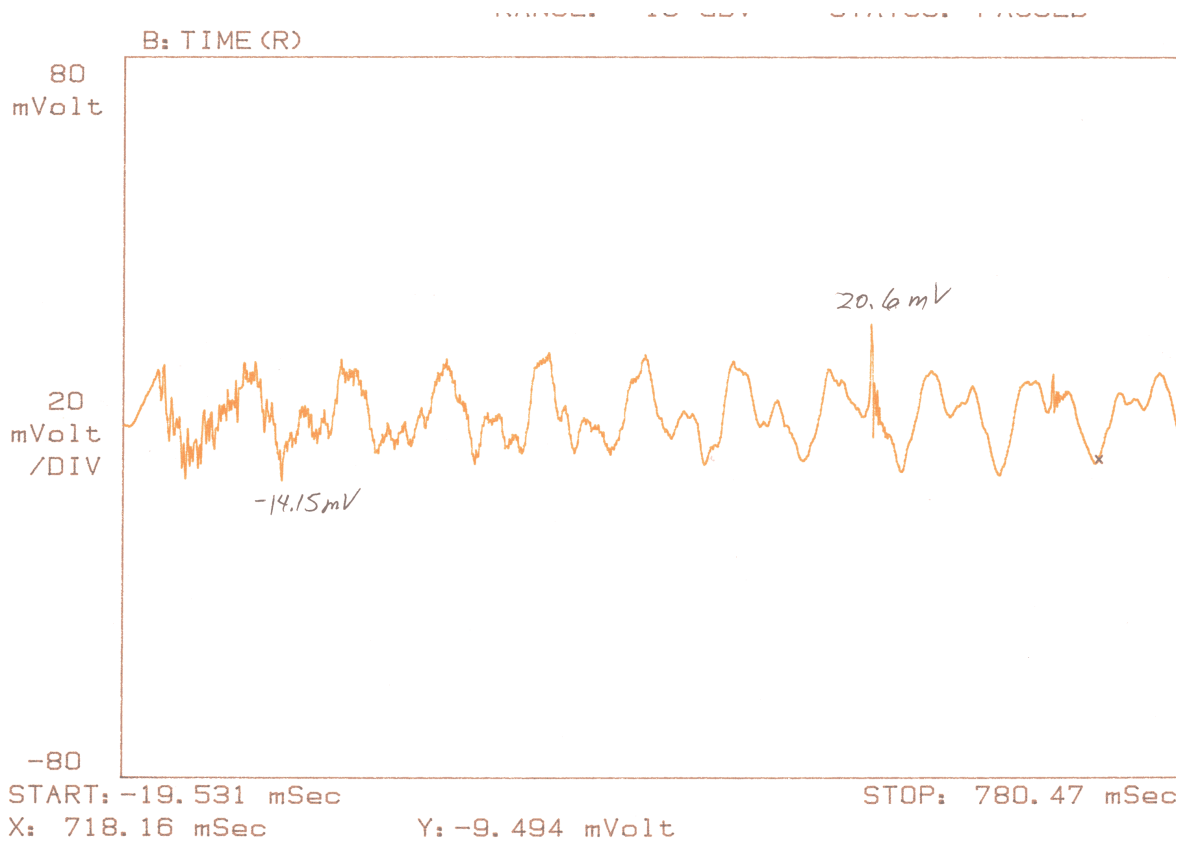


Figure 7: Target vibration measured with the target fully inserted in its low energy position inside the inner conductor of the horn 1 prototype. The 20.6mV transient corresponds to the time of the pulsing of the horn. This corresponds to a movement of about $2.5\mu\text{m}$ of the target core at a point 15.5cm downstream of the target canister.

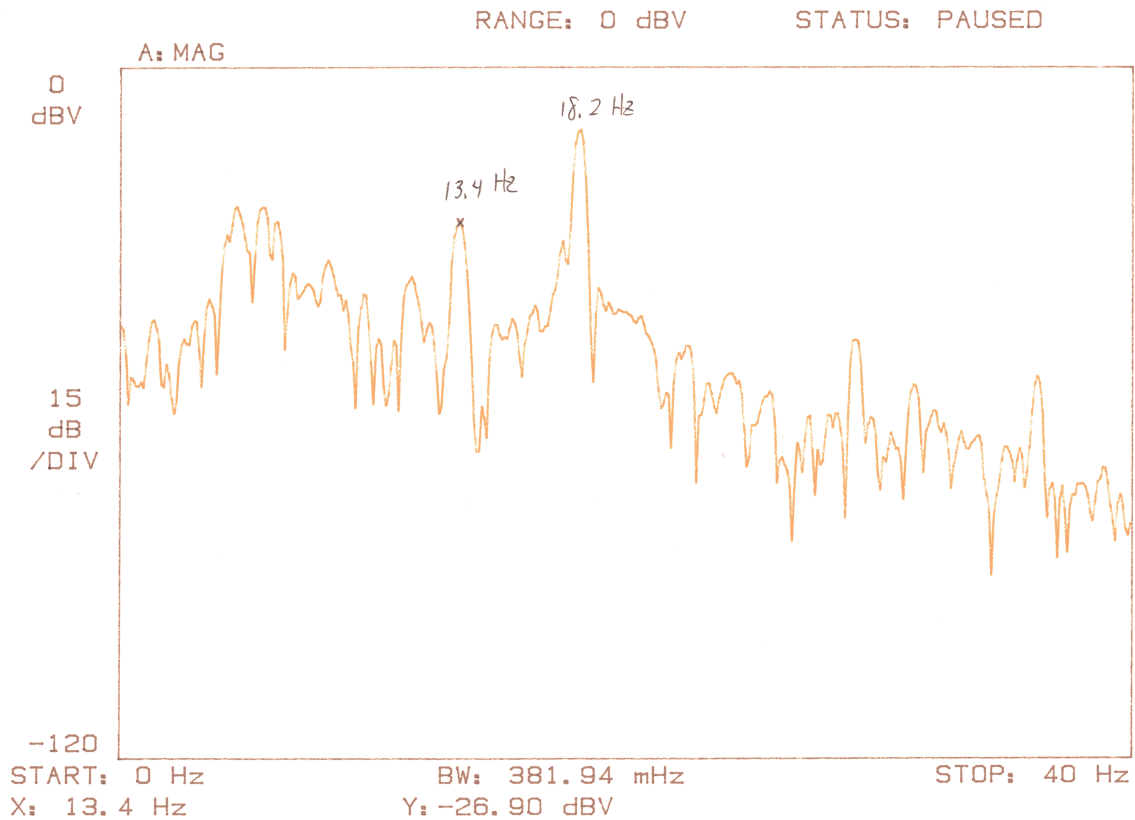


Figure 8: Target vibration frequency spectrum measured 3 cm from downstream end of target aluminum casing for the case of air flow through the target carrier supplied by two exhaust fans. The 18.2Hz peak corresponds to the vertical vibration resonant frequency. The 13.4Hz peak is the horizontal resonant frequency. This measurement was made without the plywood baffle in the bottom of the target carrier and with the target rotated 90° from its normal orientation.

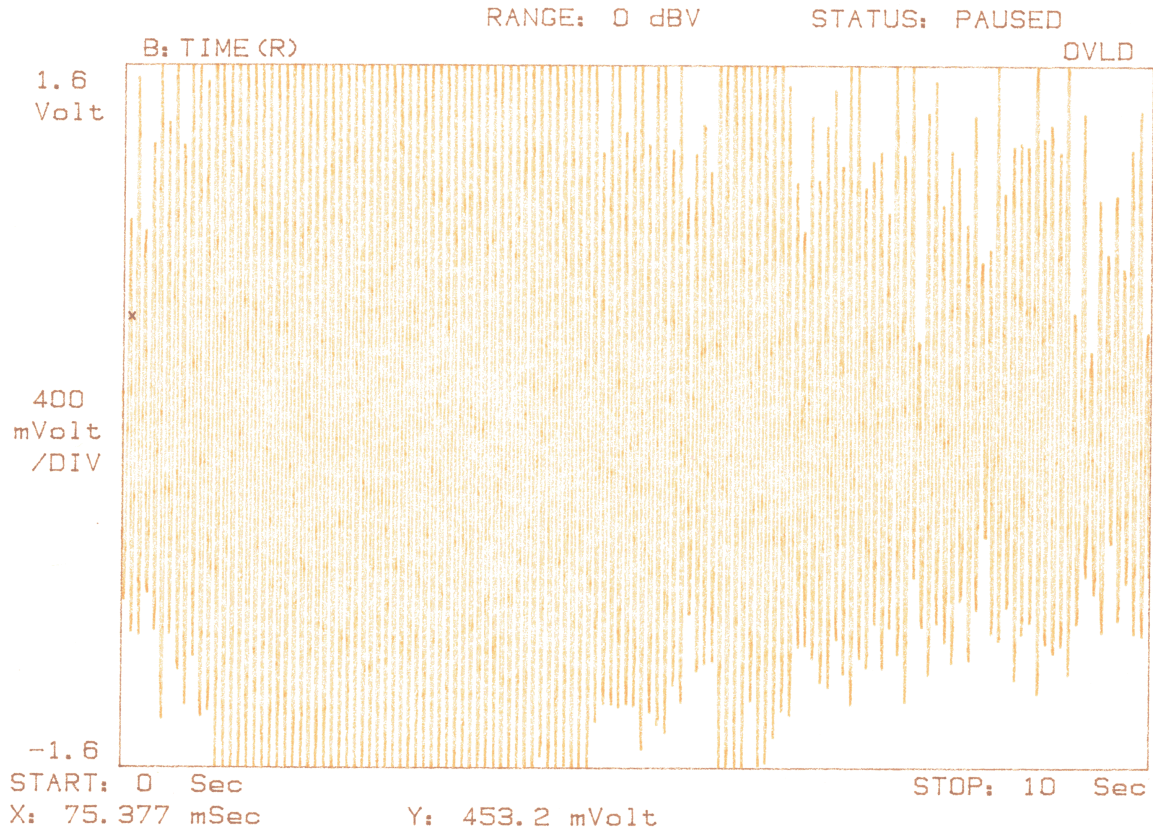


Figure 9: Target vibration measured 3 cm from downstream end of target aluminum casing. The vibration was induced by air flowing through the target carrier and deflected toward the target with plywood baffles inserted in the bottom of the carrier. The vibration is generally larger than the linear range of the eclipsometer and was estimated to be about ± 0.5 mm using a metal ruler to visually observe the vibration amplitude.

was perhaps 30° from this nominal orientation. As discussed shortly, when the water lines were connected and vibration from these checked, the air flow measurement was repeated with the proper orientation of the target. No major difference was seen in the amplitude of vibration due to air flow between these two orientations.

With the baffles in place and the target rotated about 30° from the nominal orientation, I measured the vibration of the target with air flowing through the carrier from the exhaust fans. Since the air was directed up at the target, vibration was relatively large; on the order of ± 0.5 mm. Although the eclipsometer was operating outside its linear region, one can get a impression of the erratic nature of the the vibration from figure 9 which is a time domain plot of the vibration recorded with the above discussed setup. While the vibration is generally larger than 0.2mm, there are significant periods when the vibration damps to less than 0.1mm. The accompanying frequency spectrum is shown in figure 10.

The vibration without the baffles was measured in both the 30° rotated orientation and in the final mounting with the target properly oriented, the water lines connected, and with the water-vacuum line utility festoon in place below the target. Since similar behavior was observed for both cases, I discuss here only the latter final setup. The vibration was measured 3.5cm from the

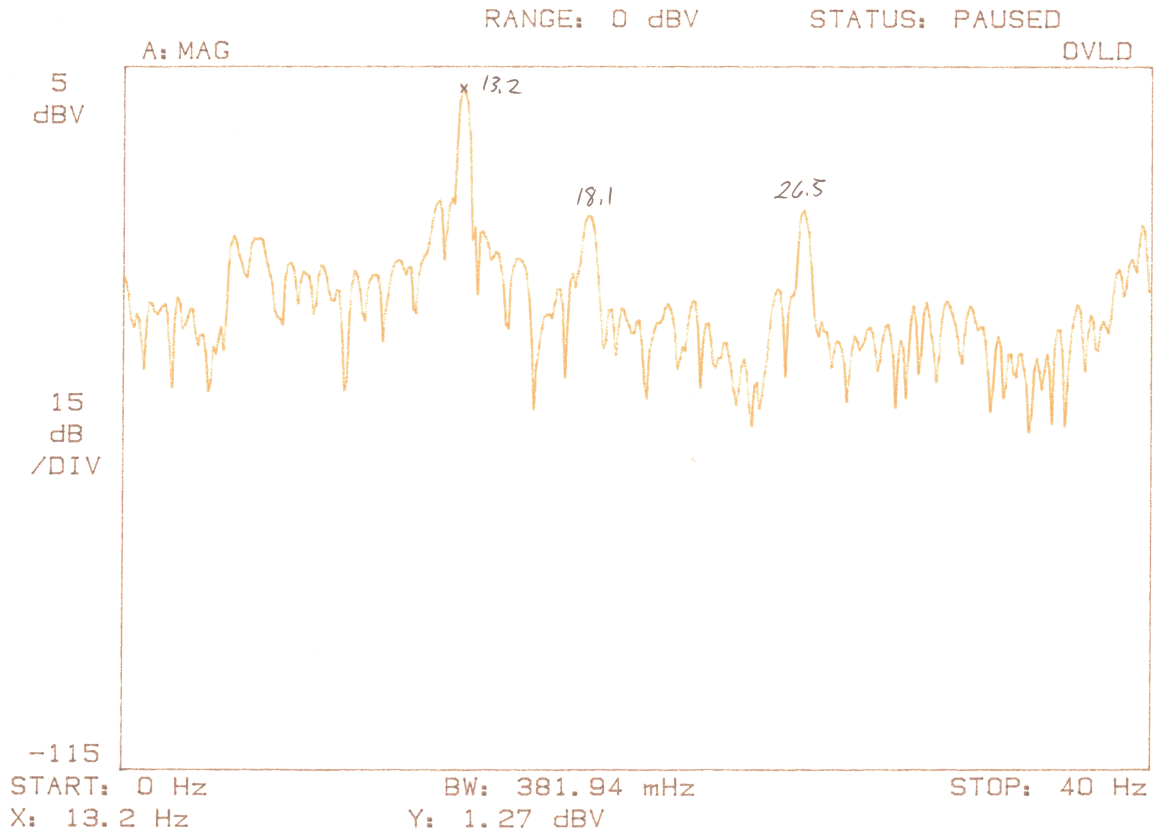


Figure 10: Target vibration frequency spectrum measured 3 cm from downstream end of target aluminum casing corresponding to the time domain measurement shown in figure 9. The fundamental horizontal and vertical frequencies of 13.2Hz and 18.1Hz are both present along with the harmonics of the 13.2Hz frequency.

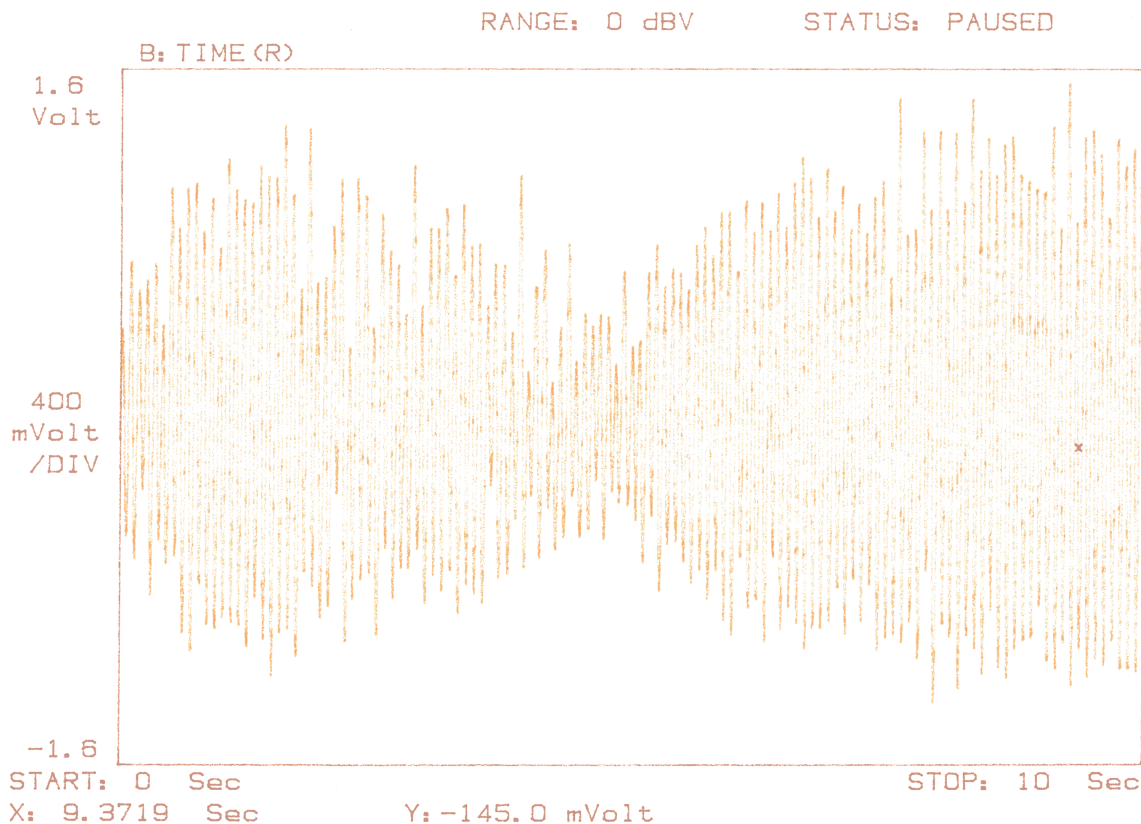


Figure 11: Target vibration measured 3.5 cm from downstream end of target aluminum casing with air and cooling water flowing. The target was mounted in the target carrier in its final position and the water-vacuum utility line festooning in the bottom of the carrier was in place.

downstream end of the target aluminum casing. Figure 11 shows the vibration recorded with both exhaust fans blowing air through the target carrier and with cooling water flowing at 3 l/min. I'll show in section 6.3 that the water causes negligible vibration. Thus, the vibration depicted in figure 11 is solely due to air flow.

The vibration is seen to be less than ~ 0.2 mm generally. There is a beat pattern that occurs randomly that damps the vibration to less than 0.07mm. The frequency spectrum is shown in figure 12. As usual, we see the 13Hz vibration and its harmonics at 26 and 39Hz; the vertical frequency now at ~ 17.5 Hz; and the second horizontal resonance at about 78Hz.

Finally, I note that during vibration measurements associated with horn pulsing (section 6.1), I also measured the vibration caused by directing a single exhaust fan at the target from a distance of about 2m. Measurements with made with the target fully withdrawn from the horn and with the target fully inserted. The fan couldn't be placed directly upstream of the target due to interference with the 3-axis transporter holding the target. The fan blew air onto the target at an angle of about 20° from the beam axis. With the fan this close to the target, it was possible to achieve a wind speed of about 9.8 m/s past the target. With the target fully withdrawn and the air hitting a "glancing blow" to the target, vibration was substantial: about ± 0.5 mm. With the target fully inserted, the horn inner conductor represented an enormous impedance to any air flow along the length of the target. The vibration at 15.7cm downstream of the target canister was measured to

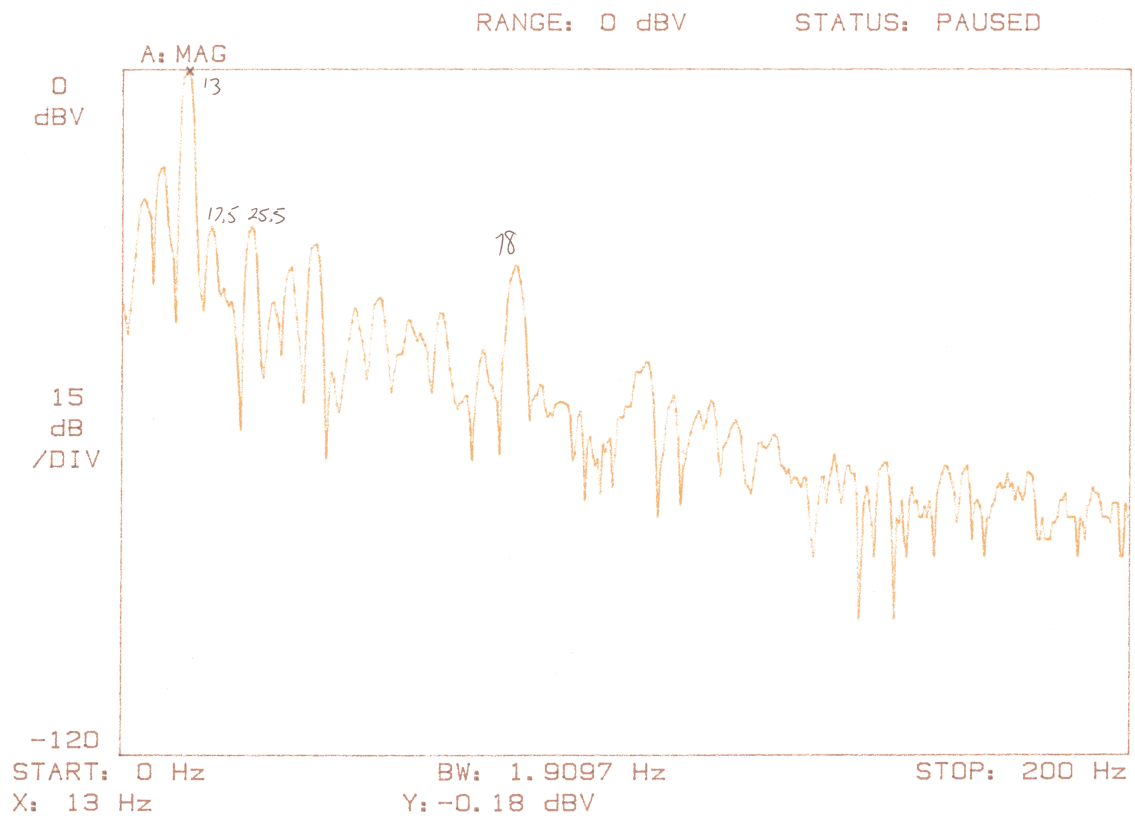


Figure 12: Target vibration frequency spectrum measured 3.5 cm from downstream end of target aluminum casing. The setup is the same as for figure 11.

be about 0.01mm. This implies vibration of less than 0.1mm at the downstream end of the target.

6.3 Vibration Measurement with Cooling Water Flow

The final test to check for environmental conditions causing target vibration was to flow cooling water through the target stainless steel support/cooling tubes at the specified rate of 3 l/min and measure any vibration caused by this. As noted in the section 6.2, this was done when the target had been installed into its final configuration in the target carrier and was carried out in parallel with the final air flow tests. The actual order of procedures was to i) take a baseline measurement with no water or air flow, ii) take a measurement with water flow only, and iii) finally, to take a measurement with both water and air flow. A measurement with air flow only was not done since, as will be evident in what follows, the water flow had negligible effect on the vibration of the target.

Figure 13 shows the time domain plot for the case of no air or water flow, and water flow only. The amplitude in the latter case is about twice that of the baseline case but still amounts to only a vibration of about $\pm 2.5\mu\text{m}$. At this level, target vibration is sensitive to mechanical vibration in the area where the measurement is being made and one can't reliably say whether the increased vibration amplitude is due to onset of water flow or to startup of some local mechanical "noise" generator. Presumably, repeated tests during a mechanically quiet period like the night-time or weekend could indicate if the source were truly the water flow. However, given the smallness of the vibration, I deemed it not worthwhile to pursue further.

For completeness, I show in figure 14, the frequency spectra for no air or water flow and for water flow only. The spectra are very similar. The 18Hz vertical mode shows up a little more clearly with water flowing and might indicate some dependence on water flow. One also sees that at this level, flicker from the fluorescent overhead building lights in MI-8 produces a prominent 120Hz peak.

7 Simulation of Target Vibration

This section will be included in a future revision of the note.

8 Conclusions

I conclude from the measurements documented here that no environmental conditions cause sufficient vibration to either change the amount of beam traversing the target or allow the target aluminum casing to contact the inner conductor of horn 1 in its low energy position. In summary, I have noted that

1. Horn pulsing induces negligible vibration in the target.
2. Cooling water flow through the target induces negligible vibration in the target.
3. Air flow past the target at a velocity similar to that expected in the target hall does cause vibration of the target if it's not inside the horn 1 inner conductor. The vibration is no greater than ± 0.5 mm. The target canister forms a large impedance to air flow in the immediate vicinity of the target aluminum casing and even with the nominal flow of 8.9 m/s through the target hall, the flow near the target casing is probably 2-3 m/s. The vibration randomly damps to small amplitude and increases again to larger amplitude.

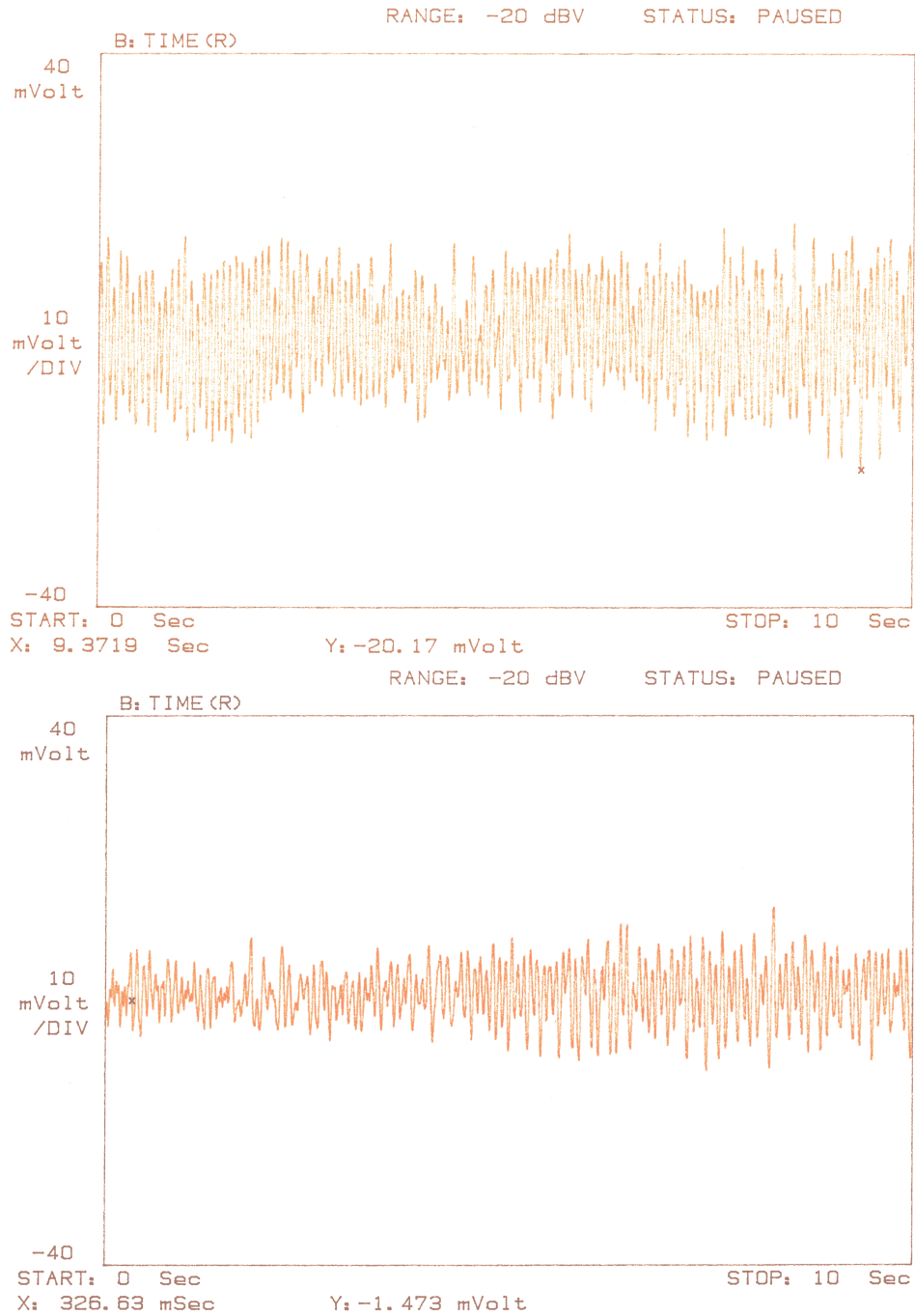


Figure 13: Target vibration measured 3.5 cm from downstream end of target aluminum casing. The lower plot is the baseline with neither air nor water flow. The upper plot is for flow of cooling water only through the target. As noted in the text, the small amplitude of vibration prohibits one from concluding that the increased amplitude in the upper plot is due to the cooling water flow.

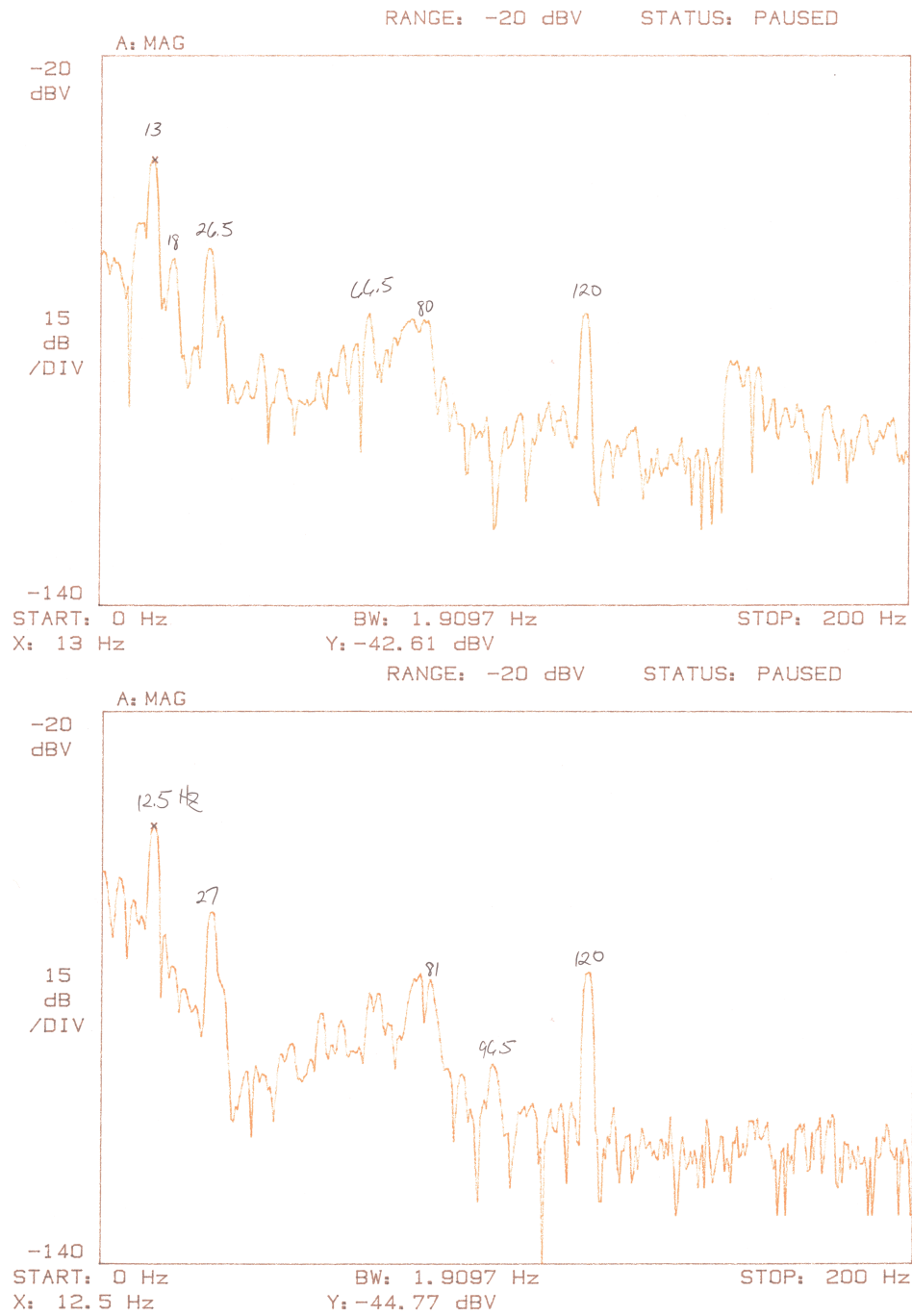


Figure 14: Target vibration frequency spectrum measured 3.5 cm from downstream end of target aluminum casing. The setup is the same as for figure 13. Lower plot is with neither air nor water flow. Upper plot is water flow only.

4. With the target inserted in horn 1, even the rapid air flow causes negligible vibration due to the dead air space the horn bore produces.

9 Acknowledgements

While I performed the measurements of vibration with the eclipsometer, the work would have been impossible to do without the help of many people. I thank Frank Nezrick for providing the eclipsometer and its accompanying support stand, positioner, power supply and dynamic signal analyzer. Hiep Le, Joe Lazzara, Willie Stitts, and Keith Gollwitzer handled all the mechanical setup in MI-8. Alberto Marchionni showed me how to operate the 3 axis transporter and the Fermilab Alignment Group patiently spent two days surveying the transporter into position and getting the target correctly positioned with respect to the horn bore. Bill Markel designed a support for attaching the target to the transporter. Kris Anderson and Jim Hysten have given many useful suggestions for carrying out the work. I am grateful for the kind assistance of them all and apologize to anyone whose help I have neglected to acknowledge.

References

- [1] The preferred source for target specifications as built is the “NuMI Technical Design Handbook”; see Sections 4.2.3 and 4.2.8 for data on the target and the target/baffle carrier. Older but useful papers on the target are the following two NuMI notes:
A. Abramov *et al.* , *Dynamic Stress Calculations for ME and LE Targets and Results of Prototyping for the LE Target*, NuMI-B-675 (10 Aug 2000).
A. Abramov *et al.* , *Advanced Conceptual Design of the Low Energy Target and Beam Plug*, NuMI-B-543 (30 Sep 1999).
- [2] K. Turvey, *Am. J. Phys.* **58**(5), 483 (May 1990).
F.S. Tse, I.E. Morse, and R.T. Hindle, *Mechanical Vibrations*, Allyn and Bacon, Boston, 1978, pp. 262-3.
- [3] Table of the ZXF-5Q graphite properties is available from Poco Graphite at web URL: www.poco.com/Graphite/zxf.asp.